

# Fabricating subwavelength dot-matrix surface structures of Molybdenum by transient correlated actions of two-color femtosecond laser beams

Jia Cong,<sup>1</sup> Jianjun Yang,<sup>1,\*</sup> Bo Zhao<sup>1</sup> and Xianfan Xu<sup>2</sup>

<sup>1</sup> Institute of Modern Optics, Nankai University, Tianjin 300071, China

<sup>2</sup> School of Mechanical Engineering, Birck Nanotechnology Center Purdue University, West Lafayette, Indiana 47907, USA

\*jjyang@nankai.edu.cn

**Abstract:** Two-dimensional matrix of subwavelength dot structures are directly generated on molybdenum surfaces by focusing two-color femtosecond laser pulses through an optical lens. In contrast to the traditional fabrication approaches, the spatial periodicities of such surface structures are demonstrated to rely on the time delay of two laser beams through transient correlation between their ultrafast dynamic processes, in spite of their different colors and polarizations. The structure orientations can be tuned effectively via the laser polarization. Discussion suggests a new possible flexible way towards the nanoscale sophisticated material processing for many potential applications.

©2015 Optical Society of America

OCIS codes: (140.3390) Laser materials processing; (220.4000) Microstructure fabrication; (260.7120) Ultrafast phenomena; (310.6628) Subwavelength structures, nanostructures.

---

## References and links

1. W. L. Barnes, A. Dereux, and T. W. Ebbesen, "Surface plasmon subwavelength optics," *Nature* **424**(6950), 824–830 (2003).
2. M. E. Stewart, C. R. Anderton, L. B. Thompson, J. Maria, S. K. Gray, J. A. Rogers, and R. G. Nuzzo, "Nanostructured plasmonic sensors," *Chem. Rev.* **108**(2), 494–521 (2008).
3. H. van Driel, J. E. Sipe, and J. F. Young, "Laser-induced periodic surface structure on solids: a universal phenomenon," *Phys. Rev. Lett.* **49**(26), 1955–1958 (1982).
4. A. Borowiec and H. K. Haugen, "Subwavelength ripple formation on the surfaces of compound semiconductors irradiated with femtosecond laser pulses," *Appl. Phys. Lett.* **82**(25), 4462–4464 (2003).
5. Reif, F. Costache, M. Henyk, and S. V. Pandelov, "Ripples revisited: non-classical morphology at the bottom of femtosecond laser ablation craters in transparent dielectrics," *Appl. Surf. Sci.* **197**, 891–895 (2002).
6. J. Bonse, M. Munz, and H. Sturm, "Structure formation on the surface of indium phosphide irradiated by femtosecond laser pulses," *J. Appl. Phys.* **97**(1), 013538 (2005).
7. A. Y. Vorobyev and C. Guo, "Femtosecond laser-induced periodic surface structure formation on tungsten," *J. Appl. Phys.* **104**(6), 063523 (2008).
8. Y. Yang, J. Yang, L. Xue, and Y. Guo, "Surface patterning on periodicity of femtosecond laser-induced ripples," *Appl. Phys. Lett.* **97**(14), 141101 (2010).
9. G. Miyaji and K. Miyazaki, "Nanoscale ablation on patterned diamondlike carbon film with femtosecond laser pulses," *Appl. Phys. Lett.* **91**(12), 123102 (2007).
10. M. Tang, H. Zhang, and T. Her, "Self-assembly of tunable and highly uniform tungsten nano gratings induced by a femtosecond laser with nano joule energy," *Nanotechnology* **18**(48), 485304 (2007).
11. N. Yasumaru, K. Miyazaki, and J. Kiuchi, "Fluence dependence of femtosecond-laser-induced nanostructure formed on TiN and CrN," *Appl. Phys., A Mater. Sci. Process.* **81**(5), 933–937 (2005).
12. Y. Yang, J. Yang, C. Liang, and H. Wang, "Ultra-broadband enhanced absorption of metal surfaces structured by femtosecond laser pulses," *Opt. Express* **16**(15), 11259–11265 (2008).
13. A. Y. Vorobyev, V. S. Makin, and C. Guo, "Brighter light sources from black metal: significant increase in emission efficiency of incandescent light sources," *Phys. Rev. Lett.* **102**(23), 234301 (2009).

14. Y. Yang, J. Yang, C. Liang, H. Wang, X. Zhu, and N. Zhang, "Surface microstructuring of Ti plates by femto-second lasers in liquid ambiances: a new approach to improving biocompatibility," *Opt. Express* **17**(23), 21124–21133 (2009).
15. J. Bekesi, J. Kaakkunen, W. Michaeli, F. Klaiber, M. Schoengart, J. Ihlemann, and P. Simon, "Fast fabrication of super-hydrophobic surfaces on polypropylene by replication of short-pulse laser structured molds," *Appl. Phys., A Mater. Sci. Process.* **99**(4), 691–695 (2010).
16. M. Huang, F. Zhao, Y. Cheng, N. Xu, and Z. Xu, "Mechanisms of ultrafast laser-induced deep-subwavelength gratings on graphite and diamond," *Phys. Rev. B* **79**(12), 125436 (2009).
17. J. Bonse and J. Krüger, "Pulse number dependence of laser-induced periodic surface structures for femtosecond laser irradiation of silicon," *J. Appl. Phys.* **108**(3), 034903 (2010).
18. T. Wang and C. Guo, "Angular effects of nanostructure-covered femtosecond laser induced periodic surface structures on metals," *J. Appl. Phys.* **108**(7), 073523 (2010).
19. J. Reif, O. Varlamova, and F. Costache, "Femtosecond laser induced nanostructure formation: self-organization control parameters," *Appl. Phys., A Mater. Sci. Process.* **92**(4), 1019–1024 (2008).
20. R. Buividas, M. Mikutis, and S. Juodkazis, "Surface and bulk structuring of materials by ripples with long and short laser pulses: recent advances," *Prog. Quantum Electron.* **38**(3), 119–156 (2014).
21. T. Jia, H. Chen, M. Huang, F. Zhao, J. Qiu, R. Li, Z. Xu, X. He, J. Zhang, and H. Kuroda, "Formation of nano-gratings on the surface of a ZnSe crystal irradiated by femtosecond laser pulses," *Phys. Rev. B* **72**(12), 125429 (2005).
22. C. Wang, H. Huo, M. Johnson, M. Shen, and E. Mazur, "The thresholds of surface nano-/micro-morphology modification with femtosecond laser pulse irradiations," *Nanotechnology* **21**(7), 075304 (2010).
23. I. B. Divliansky, A. Shishido, I.-C. Khoo, T. S. Mayer, D. Pena, S. Nishimura, C. D. Keating, and T. E. Mal-louk, "Fabrication of two-dimensional photonic crystal using interference lithography and electrodeposition of CdSe," *Appl. Phys. Lett.* **79**(21), 3392–3394 (2001).
24. H. Misawa, T. Kondo, S. Juodkazis, V. Mizeikis, and S. Matsuo, "Holographic lithography of periodic two- and three-dimensional microstructures in photoresist SU-8," *Opt. Express* **14**(17), 7943–7953 (2006).
25. M. Kirillova, L. Nomerovannaya, and M. Noskov, "Properties of molybdenum single crystals," *Sov. Phys. JETP* **33**(6), 1210–1214 (1971).
26. S. Höhm, A. Rosenfeld, J. Kruger, and J. Bonse, "Femtosecond diffraction dynamics of laser-induced periodic surface structures on fused silica," *Appl. Phys. Lett.* **102**(5), 054102 (2013).
27. Q. Gan, Y. J. Ding, and F. J. Bartoli, "Rainbow" trapping and releasing at telecommunication wavelengths," *Phys. Rev. Lett.* **102**(5), 056801 (2009).
28. Z. Han, C. Zhou, E. Dai, and J. Xie, "Ultrafast double pulse ablation of Cr film on glass," *Opt. Commun.* **281**(18), 4723–4726 (2008).
29. M. Huang, Y. Cheng, F. Zhao, and Z. Xu, "The significant role of plasmonic effects in femtosecond laser-induced grating fabrication on the nanoscale," *Annalen Der Physic.* **525**(1-2), 74–86 (2013).

## 1. Introduction

Micro/nano-structuring metallic surfaces has attracted great attention as a means of modulating material surface properties to control interactions without chemical styles, which provides bright prospects for the fundamental researches and wide possible applications ranging from novel optical devices to biological sensors [1,2]. Although the mature technology of lithography has been successfully employed for such material processing, this kind of top-down approach often possesses complex procedures under restricted conditions by requiring the mask designs and photoresists. Alternatively, self-assembly of periodic grooves with micro and nano scales can be realized by means of laser irradiation, producing so-called Laser-Induced Periodic Surface Structures (LIPSS) in a mask-free, single-step process that may be considered as bottom-up approach [3,4]. This technique has been already carried out on a variety of materials including metals, semiconductors and dielectrics especially at the energy fluence near the damage threshold [5–11], which might give potential routes to laser processing beyond the diffraction limit. More interestingly, such laser induced micro/nano-structures have been identified to modify the properties of material surfaces, providing wide applications in many areas such as the enhanced optical absorption [12], the improved thermal or field emission [13], the increased hydrophobicity and biocompatibility [14,15].

Generally, the formation of LIPSS strongly depends on material properties as well as the incident laser conditions including the wavelength ( $\lambda$ ) [16], the pulse energy and the number of pulses [17,8], and the polarization state [18,19]. The achieved periodicity ( $\Lambda$ ) can be categorized into low spatial frequency and high spatial frequency. For the incident linearly polarized femtosecond laser on highly absorbing materials such as metals, LIPSS orientation can

be either perpendicular or parallel to the laser polarization direction [20]. The physical mechanisms are commonly attributed to interference between the incident laser light and excited surface plasmon polaritons (SPPs) [3,5,8,16]. Apart from this, some other possible explanations have also been suggested [2,21,22]. Remarkably, aiming at the wider application of LIPSS, some researchers have recently developed two-dimensional (2D) periodic surface structures by adopting a holographic multi-beam interference method with a single color femtosecond laser [23,24]. This approach, however, is in fact a direct simple ablation of material surfaces on the selected areas with the patterned laser intensities, which possesses some defects in fabrication flexibility and structure controlling.

In this paper, by applying two-color femtosecond laser pulses (800 nm Ti:sapphire laser and its second harmonic wavelength of 400 nm), we produce 2D dot-matrix structures on metallic bulk molybdenum (Mo) surfaces in a single irradiation step. Different from the traditional method, the periodicity of the matrix structures can be controlled through correlating the two different transient states of laser-matter actions. Further experiments reveal the significance of the temporal delay between two-color laser beams on the formation of surface structures. Based on these results, we finally discuss the underlying mechanisms.

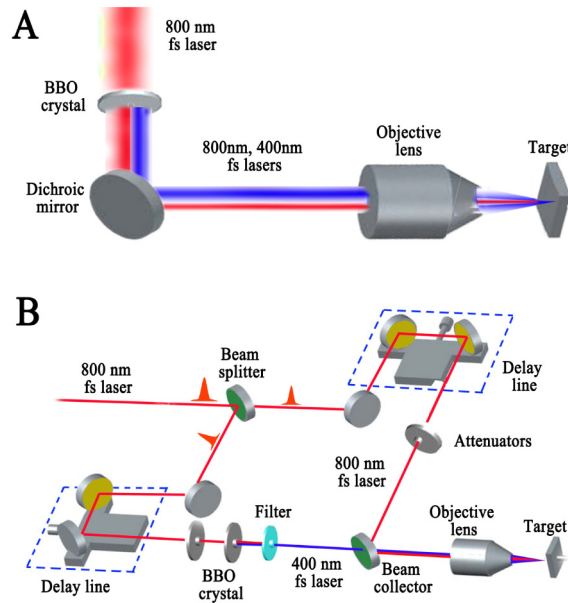


Fig. 1. Schemes of the experimental setup for fabricating dot-matrix structures on the metal surfaces. (a) By direct irradiating collinear two-color femtosecond laser beams; (b) By irradiating temporally delayed collinear two-color femtosecond laser beams.

## 2. Direct irradiating collinear two-color femtosecond laser beams

A commercial chirped pulse Ti:sapphire regenerative laser amplifier system (Spectra Physics HP-Spitfire 50) was used to generate linearly polarized laser pulses, with the central wavelength  $\lambda = 800$  nm operating at the repetition rate of 1 kHz. The pulse time duration is 50 fs and the single pulse energy is 2 mJ. This laser was frequency-doubled by second harmonic generation (SHG) in a 1 mm thick, type-I ( $o + o \rightarrow e$ ) cut, beta barium borate (BBO) crystal to generate a collinear propagation of two-color femtosecond laser beams, including the fundamental center wavelength 800 nm and the SHG center wavelength 400 nm. Then they were reflected by a dichroic mirror (reflectivity less than 5% for 800 nm but larger than 60% for 400 nm) towards into an objective lens ( $4 \times$ , N.A. = 0.1) for the beam focusing. A polished Mo plate (1 mm thickness) was mounted on a computer-controlled three-axis ( $x,y,z$ ) translation

stage (New Port UTM100 PPE1), whose optical indexes are  $n = 3.46$  and  $2.66$  for the laser wavelengths of  $800\text{ nm}$  and  $400\text{ nm}$ , respectively [25]. The sample surface was orientated perpendicular to the optical axis. The experiment was carried out by a line-scribing method under the fixed irradiation of lasers. Details of the setup can be seen in Fig. 1(a). The sample surface was slightly moved away from the focus to avoid strong ablation damage, which allows the laser spot on the target to exhibit a Gaussian fluence distribution with a  $(1/e^2)$  diameter of  $30\text{--}40\text{ }\mu\text{m}$ . Before and after the experiments, the sample surface was ultrasonically cleaned in acetone solution.

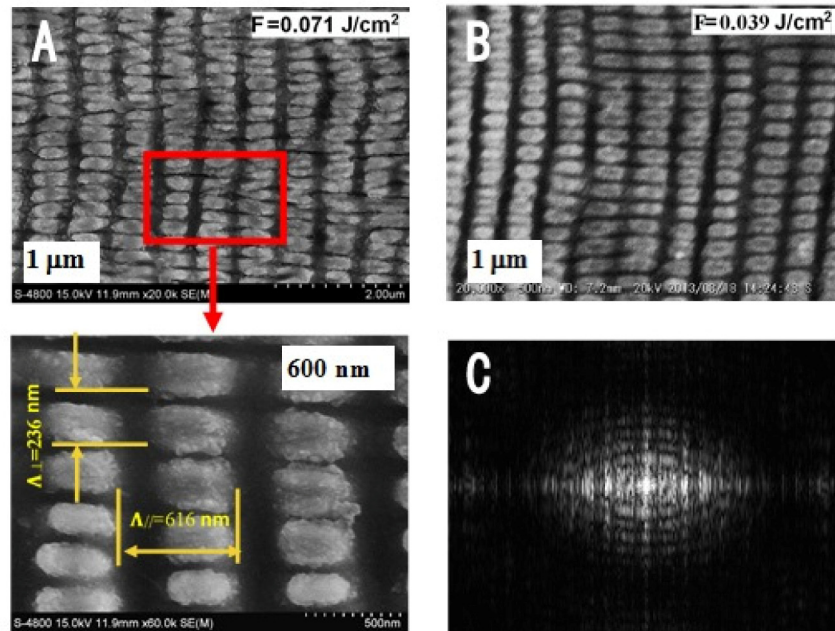


Fig. 2. (a)–(b) SEM images of the subwavelength dot-matrix structures on Mo surfaces by direct irradiating collinear two-color femtosecond laser beams at energy fluences of  $F = 0.071\text{ J/cm}^2$  and  $F = 0.039\text{ J/cm}^2$ , respectively; (c) 2D Fourier transformation of SEM image in Fig. 2(a).

First, the nonlinear crystal was set to fulfill the phase-matching condition, resulting in the output of orthogonal linear polarization of two-color femtosecond laser beams. Figures 2(a)–2(b) show scanning electron microscopy (SEM) images of the surface structures obtained respectively at two-color laser peak energy fluences of  $F = 0.071\text{ J/cm}^2$  and  $0.039\text{ J/cm}^2$ , where the energy ratio ( $F_{\lambda = 400\text{nm}}/F_{\lambda = 800\text{nm}}$ ) of two laser wavelengths is 3, and the scanning speed is  $0.04\text{ mm/s}$ , equivalent to the number of overlapping pulses per-micrometer of about 25. Clearly, these images represent 2D periodic arrays of surface structures on the laser irradiation areas. In a zoom-in picture of Fig. 2(a), we can see that the structure periodicity in the horizontal direction is much different from that in the vertical direction with  $\Lambda_{\parallel} = 616\text{ nm}$  and  $\Lambda_{\perp} = 236\text{ nm}$ , respectively. Such structures can be recognized as a regular matrix of metallic elongated subwavelength dots on the sample surfaces. Moreover, the spatial periodicity of the structures has been investigated by discrete two-dimensional fast Fourier transformation, as shown in Fig. 2(c), in which the distinct bright spots in two dimensions actually reflect the regularity of the metallic dot arrangement along both horizontal and vertical directions.

With a large quantity of experimental measurements, we can obtain a dynamic range for the large-scale formation of the dot-matrix surface structures in terms of the laser fluence and the scanning speed. For example, given the two-color laser fluence within a range of  $F =$

0.07-0.11 J/cm<sup>2</sup>, the appropriate scanning speeds are varied from 0.01 mm/s to 0.04 mm/s; while if the laser fluence increases to  $F = 0.11\text{-}0.25$  J/cm<sup>2</sup>, the appropriate scanning speeds become larger than 0.1 mm/s. However, at the two-color laser fluence of  $F > 0.25$  J/cm<sup>2</sup>, the regular matrix structures were no longer formed within our speed range. In particular, this kind of surface structure not only depends on the total incident laser fluence but also strongly influenced by the energy ratio between the two laser components. The measured optimal energy ratios of the two laser components are 2.9~5.8. In addition, we also investigated the structure periodicity variations in two dimensions as a function of the scanning speed at the given two-color laser fluence, as shown in Fig. 3. The periodicity along the vertical direction is relatively small with a dynamic range of about  $\Lambda_{\perp} = 220\text{-}300$  nm; while the periodicity along the horizontal direction has relatively large values with a dynamic range of about  $\Lambda_{\parallel} = 570\text{-}690$  nm.

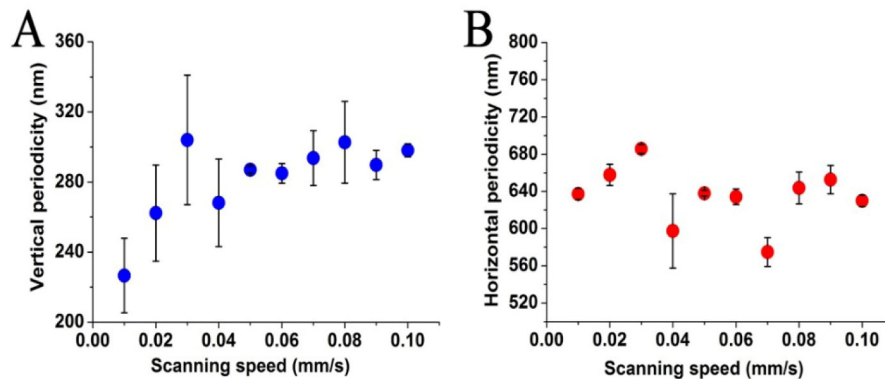


Fig. 3. Measured scanning speed dependence of the matrix structure periodicities in two dimensions at the given laser fluence of  $F = 0.07$  J/cm<sup>2</sup>. (a) In the vertical direction; (b) In the horizontal direction. Each data was obtained from three different positions of each SEM image and then averaged over two experiments, and the error bars represent statistical fluctuations during the measurements.

In the experiments, with gradual deviating the azimuth angle of BBO crystal from its full phase-matching condition, the SHG signal can keep its linear polarization but with alterable directions, while the residual infrared (IR) signal becomes elliptically polarized (here  $\theta = 0^\circ$  corresponds to the azimuth angle of the crystal at the full phase-matching condition, and  $\theta > 0^\circ$  represents its anti-clockwise rotations). Under such circumstances, the matrix-ordered dot surface structures can only take place within a range of  $-35^\circ < \theta < 35^\circ$ . Otherwise, it will become trivial and even disappear completely. Figures 4(a)–4(b) show the typical results obtained at the crystal azimuth angles of  $\theta = -25^\circ$  and  $\theta = 35^\circ$ , respectively. Evidently, in the both cases the alignment of surface structures appears to slant but into opposite directions. When referring to the matrix orientations at  $\theta = 0^\circ$ , the measured structure orientation variations for either the large or the small periodicity are illustrated in Fig. 4(c), where the maximum slantwise angles for two periodicity orientations can reach as large as  $\pm 60^\circ$ . Furthermore, the individual metallic dots are observed to change in size during the orientation slant. This phenomenon is physically attributed to the polarization change of two-color lasers during the rotation of BBO crystal, suggesting a convenient way to modify the matrix structures.

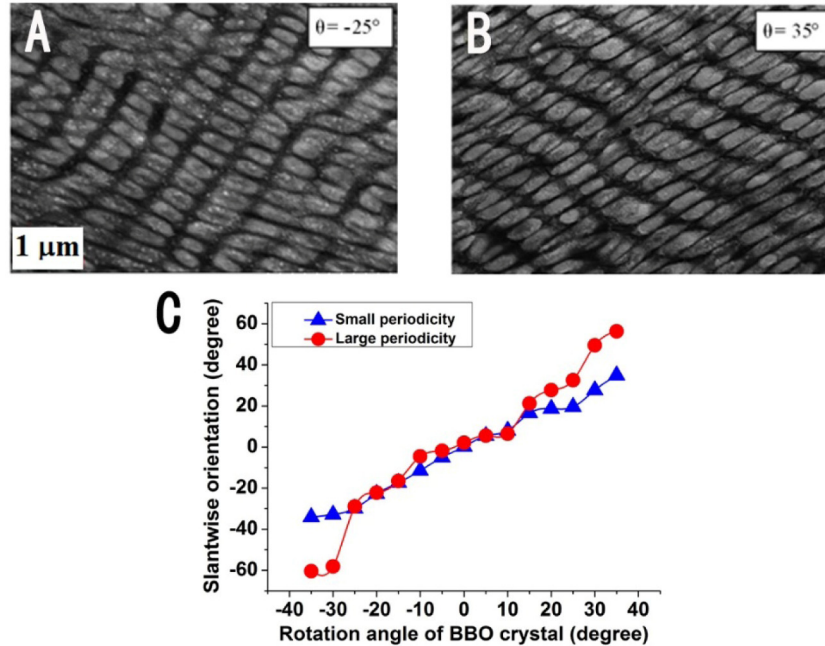


Fig. 4. (a)–(b) Slantwise oriented dot-matrix surface structures at two-color laser fluence of  $F = 0.07 \text{ J/cm}^2$  when the azimuth angle of BBO crystal is  $\theta = -25^\circ$  and  $\theta = 35^\circ$ , respectively; (c) Measured slantwise angles of two orientations for the matrix surface structures as a function of rotating BBO crystal.

At the first glance, the aforementioned dot-matrix surface structures are constituted by the simple intersecting two fs-LIPSSs that are respectively from laser pulses of 800 nm and 400 nm wavelengths. To prove this intuitions, we obtained two individual femtosecond laser beams using color filters, and their own LIPSSs are formed on two separate surface regions under the same laser fluence of  $F = 0.07 \text{ J/cm}^2$ , as shown in Figs. 5(a)–5(b), where the measured LIPSS periodicities for the IR and blue laser beams are  $\Lambda = 589 \text{ nm}$  and  $300 \text{ nm}$ , respectively. Moreover, when the two individual laser beams were irradiated one after another on the same surface region by two separate scanning steps, only one-dimensional (1D) fs-LIPSS can be achieved. To be more specific, LIPSS in the first-step scanning process was washed out and replaced by that in the second-step scanning process. On the other hand, when two-color laser spots were spatial partially overlapped on the sample surface, the formation of surface structures appeared different with either upward or downward scanning process, as shown in Figs. 5(c)–5(d). In the former case, the matrix-ordered dot surface structures can still be fabricated; while in the latter case only 1D LIPSS that are originated from the IR laser pulse can be observed. This result indicates that a certain temporal delay irradiation of the blue laser beam is very necessary for the formation of dot-matrix surface structures. As a matter of fact, in the experiment setup of Fig. 1(a) with the positive dispersion of the optical elements, the blue laser beam was eventually time-delayed to arrive onto the sample with respect to the IR laser beam. These analyses will be further confirmed by the following experiments.



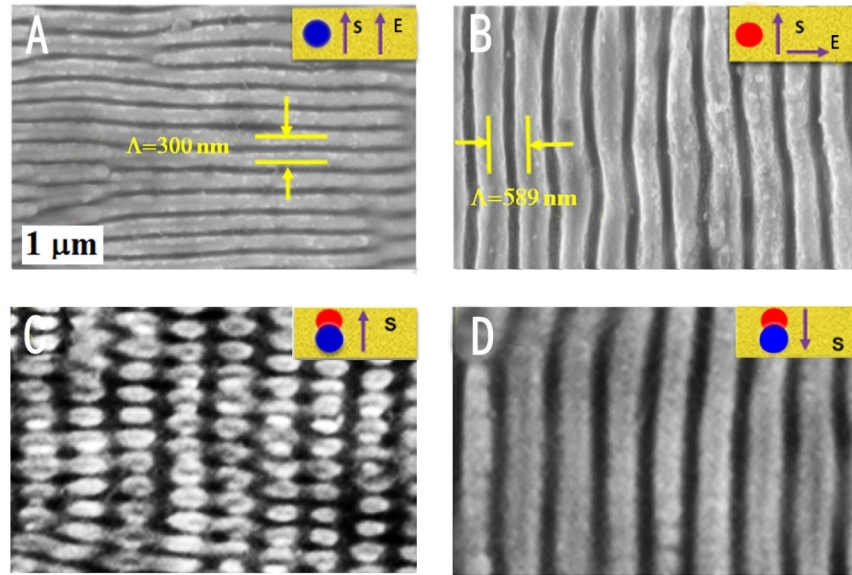


Fig. 5. (a)–(b) SEM images of surface structure induced by two individual femtosecond laser beams centered at wavelength of 400 nm and 800 nm, respectively; (c)–(d) Surface structures obtained by scanning of partially overlapped two-color laser spots in either upward or downward direction, respectively. In the inset pictures, red and blue spots represent femtosecond laser beams centered at 800 nm and 400 nm wavelengths, respectively. S and E respectively indicate the directions of the laser scanning and the laser electric field.

### 3. Irradiating temporally delayed two-color femtosecond laser beams

In this case, the IR femtosecond laser pulses delivered from the Ti:sapphire amplifier system were transformed by a Michelson interferometer into fs-pulse pairs of nearly equal energies. BBO crystal was inserted into one arm and 400 nm wavelength pulses were finally obtained through color filters, whose linear polarization was adjusted to the vertical direction by a half wave-plate. The femtosecond laser in the other arm was maintained in both wavelength and the horizontal linear polarization. A temporal delay ( $\Delta t$ ) of the two arms was adjusted between  $-330$  ps and  $+330$  ps (positive delay times indicate the arrival of IR pulse prior to blue pulse), and their pulse energies were varied separately by neutral density filters. Two-color laser beams were finally collected into collinear propagation and focused through an objective lens onto the sample surface. Details of the setup are shown in Fig. 1(b).

Figure 6 shows the evolution of surface structures with the delay time of two-color femtosecond laser beams, where their energy fluences are given respectively by  $F_{\lambda=800\text{nm}} = 0.07$  J/cm<sup>2</sup> and  $F_{\lambda=400\text{nm}} = 0.14$  J/cm<sup>2</sup> under the scanning speed of 0.04 mm/s. At the negative delay times of  $\Delta t \leq -50$  ps, only 1D LIPSS with vertical orientation was observed on the sample surface, which suggests the prevailing action of the delayed 800 nm laser beam. As the negative delay time reduced to  $\Delta t = -30$  ps, there emerged an embryonic form of matrix-ordered dot surface structures, indicating the LIPSS of the priorly irradiated blue laser beam. In this case, the metallic dots are arranged in closely along the vertical direction to show a large duty cycle. At the delay time of  $\Delta t = -5$  ps, the dot-matrix surface structures became more apparently. Especially as the delay time entered into a positive region of  $0 < \Delta t < 40$  ps, the well-organized matrix structures become more pronounced, similar to observations in the direct irradiation experiments. More interestingly, as the delay time was  $\Delta t = 40$ –50 ps, the structure periodicity along the vertical direction suddenly decreased by half, suggesting the interplay of two laser beams. However, this behavior began to change at the positive delay time of  $\Delta t =$

50-85 ps, in which the typical dot-matrix surface structures was regained. Surprisingly, as the delay time reached  $\Delta t = 90-190$  ps, the structure periodicity along the horizontal direction was decreased by half but it kept invariant along vertical direction, revealing a modification by the temporally delayed blue laser pulse. Such change tendency seems to be reversal of the observation in  $\Delta t = 40-50$  ps. If the delay time continued to increase into a regime of  $\Delta t = 200-240$  ps, the surface morphology was inclined to recover the dot-matrix features but accompanied by a gradual fading away of periodicity in the horizontal direction. Finally, when the delay time became large than  $\Delta t = 250$  ps, only horizontally orientated LIPSSs were obtained on the sample surface, with severe shrinking spatial periodicity into the deep subwavelength regime.

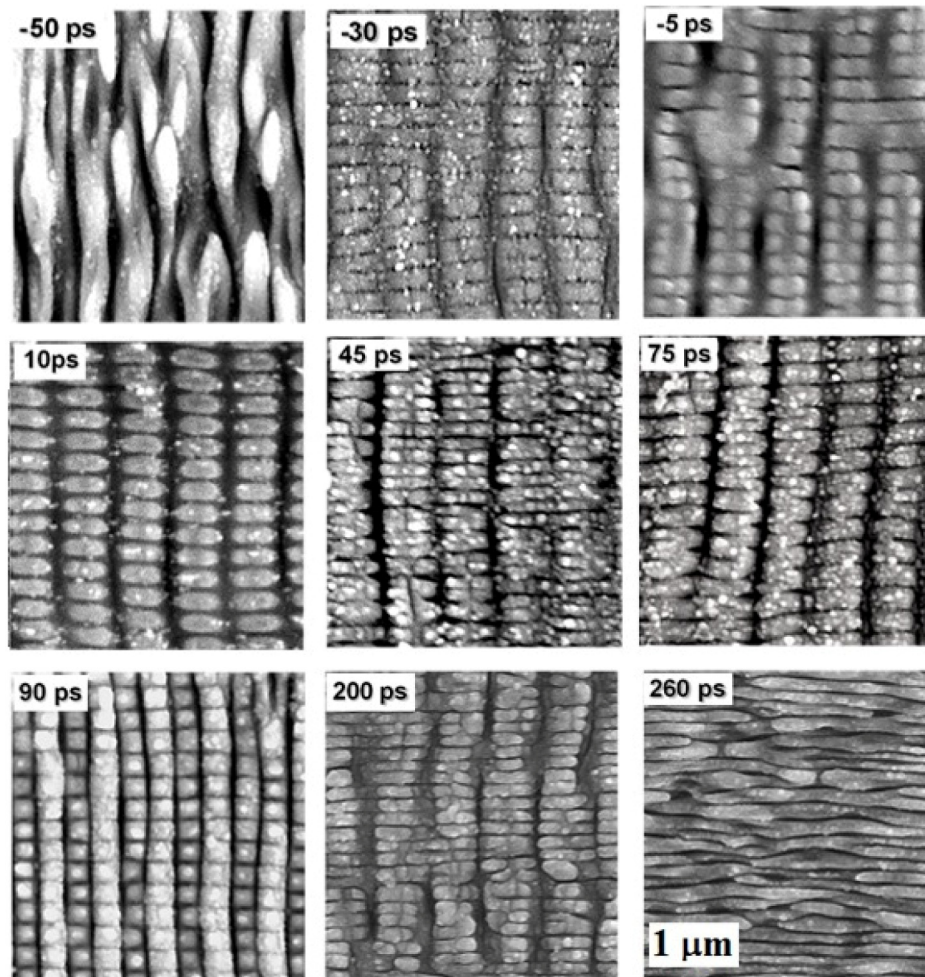


Fig. 6. Variable surface structures induced by two-color femtosecond laser pulses with different delay times (here positive delay times represent the arrival of the IR laser pulse prior to the blue laser pulse, and the sample scanning is along the horizontal direction).

Then the experiment was repeated with changing either the total energy or the energy ratio between the two-color laser beams, and the similar dependence of the periodicity on the delay time was found but with different critical times for the structural changes, which becomes larger for the higher laser energy or their energy ratio approaching to the unity. To obtain deep insights into the surface structure evolution shown in Fig. 6, we measured varia-



tions of structure periodicity in two dimensions as a function of the delay time, as depicted in Fig. 7. Along the the vertical direction, the structure periodicity firstly demonstrates a trend of slow increase to approximate  $\Lambda = 270$  nm within the negative delay time regime, and then presents a tendency of dramatical reduction to about  $\Lambda = 150$  nm nearby the delay time  $\Delta t = 50$  ps. After a short delay-time period (about 10 ps), the vertical periodicity rapidly recovers to about  $\Lambda = 260$  nm and then drop gradually down to  $\Lambda = 140$  nm during the delay time range of  $\Delta t = 70$ -300 ps. While along the horizontal direction, the structure periodicity firstly displays a fast increasing tendency form  $\Lambda = 350$  nm to about  $\Lambda = 650$  nm during the negative delay time regime, and there is almost no change in the delay time range of  $\Delta t = 0$ -90 ps. Then it suddenly falls by half into a new regime of  $\Lambda = 340$  nm during the delay time of  $\Delta t = 90$ -150 ps. After that, it begins to increase gradually to  $\Lambda = 700$  nm at the delay time of  $\Delta t = 230$  ps. For the larger delay times, the structure periodicity in the horizontal direction will become absent. From these results, we conclude that two-color femtosecond laser beams can have mutual correlations during their own LIPSS formation dynamics if the appropriate delay time is adopted.

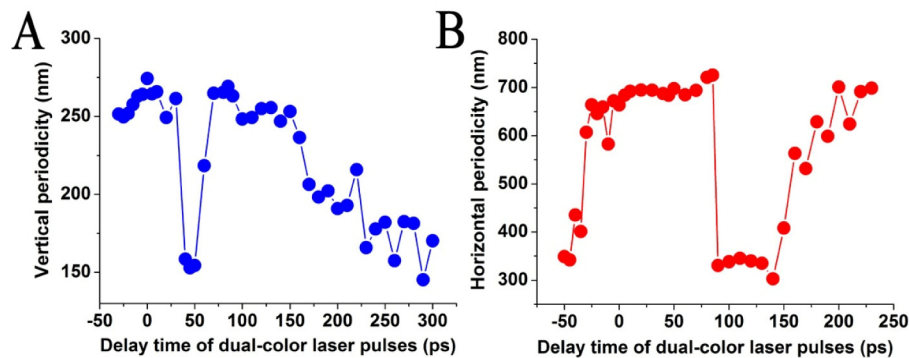


Fig. 7. Measured variations of the periodicity in two dimensions as a function of the delay time between two-color laser beams. (a) In the vertical direction; (b) In the horizontal direction.

The following scenario try to elucidate the underlying mechanisms of the experimental observations: when a femtosecond laser beam is incident on the metal surface, its interference with the excited surface plasmons results in spatially periodic energy distribution patterns that run perpendicular to the laser electric field [6–18]. The initial nonuniform energy deposition will be first absorbed by electrons and then transferred to the lattice through the electron-phonon coupling, leading to the periodic removal of materials, termed as LIPSS topography, on the surface if the lattice temperature is heated above the ablation threshold. In the case of two-color femtosecond laser beam irradiation, the prior pulse arriving at the sample first imprints periodic regions with different optical properties on the pristine material surface, or a transient index grating can be formed [26], whose spatial periodicity depends on the incident laser wavelength. For the negative delay-time irradiations, the transient grating that is determined by the prior incident shorter wavelength pulse has a relatively small periodicity. Through considering the fact of thermal expansion in the metal, such small-periodicity transient grating-like patterns are more likely to have a spatial coalescence each other, leading to the disappearance of the 2D surface structures. This effect becomes pronounced for the well-defined prototype of LIPSS owing to the enhanced optical absorption. Therefore, the larger the negative delay time, or the higher the temporally delayed laser intensity, the more serious the thermal expansion of the transient index grating will become. This can be illustrated by Fig. 8. On the other hand, for the positive delay-time irradiations where the longer wavelength pulse interacts with the material first, the induced transient refractive grating turns to

have relatively large periodicity. Therefore, the spatial coalescence of such large-periodicity transient grating-like patterns can take place at longer delay times.

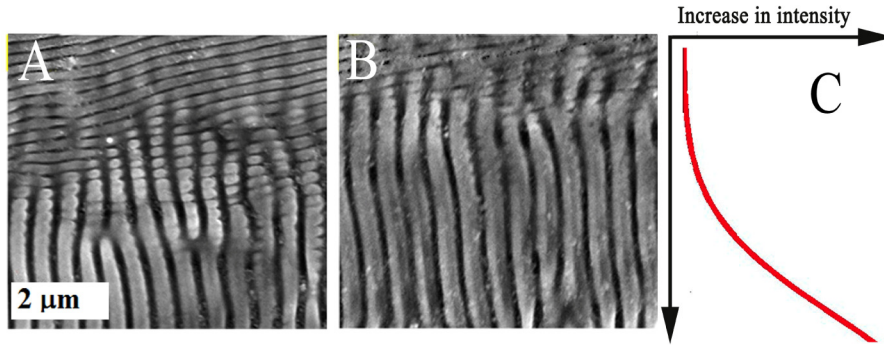


Fig. 8. Observed dynamic coalescence of the prior ripple structure under the irradiation of femtosecond laser beam with different delay times. (a)  $\Delta t = -15$  ps; (b)  $\Delta t = -30$  ps. The horizontally orientated ripple structures are generated by the prior incident blue femtosecond laser beam, and the vertically orientated ripple structures are generated by the delayed incident IR femtosecond laser beam. (c) The sketch of intensity distribution of the temporally delayed incident femtosecond laser beam in space along the vertical direction.

In Fig. 8, since the temporally delayed incident femtosecond laser beam gives a Gaussian intensity distribution in space [Fig. 8(c)], its subsequent action on the already existent ripple structures become spatially dependent. As shown in Fig. 8(a), the horizontally orientated LIPSS seems to be almost untouched in the lower laser intensity areas, but it breaks into some isolated dots in the increased laser intensity areas, constituting -ordered topography. Noticeably, in the higher intensity areas the spatially isolated metallic dots along the vertical direction begin to disappear, and they are replaced by the vertical alignment of continuous stripes, suggesting the washout or coalescence of the horizontal LIPSSs by the time-delayed IR femtosecond laser beam. Figure 8(b) shows that such spatial coalescence of the metallic dots along the vertical direction becomes more pronounced when the delay time of two laser beams increases. Now we can understand why the dot-matrix structures were degraded with larger delay times.

For the positive delay time cases, when the temporally delayed blue laser beam arrives, there already exists a transient index grating on the metal surface that was triggered by the previously incident IR laser beam, which can subsequently modify the excitation of surface plasmons. With electron-phonon coupling and electron diffusion in the tens-picosecond scale, the crystalline lattices of the transient index grating tend to have the higher temperature and larger depth, which modify the dielectric function of the sample surface and consequently make the excitation of surface plasmon decrease in the wavelength [27]. In our experiments, the sudden reduction of the periodicity along the vertical direction nearby  $\Delta t = 50$  ps can be attributed to this physical effect. Beyond this delay time, thermodynamic effects start to degrade the grating temperature, and the surface deformation or roughness begins to play an important role with increasing the delay time. The more rough the surface, the smaller the LIPSS periodicity will be [8]. As a result, the gradual decreasing vertical periodicity was observed within the delay time of  $\Delta t = 70$ -300 ps. On the other hand, variations of the structure periodicity from the prior incident IR laser pulse are also modulated by the delayed incident blue laser beam. At the shorter negative delay times, the elevated electron/lattice temperature on the metal surface from the prior blue laser beam was re-improved by the temporally delayed incident IR laser beam (although their wavelengths and polarizations are different), being equivalent to the absorption of more laser energies [28]. Therefore, the final electron/lattice temperature will be higher at shorter delay times, resulting in larger periodicity of the temporally delayed IR laser beam. Such behavior is also applied for the observed varia-

tion of the vertical periodicity at negative delay times. As the delay time enters into the range of  $\Delta t = 90\text{-}150$  ps, the instability caused by the thermal diffusion depth and dielectric constant altering take place for the transient index grating and especially is strengthened under the irradiation of delayed blue laser beam. According to the previous study [29], this physical effect unavoidably results in the grating splitting processes, so that the final structure periodicity along the horizontal direction reduces by half. Beyond this delay time range, the lattice temperature of the metal surface is decreased with larger temporal separation of two-color laser beams, which leads to a gradual increase of the horizontal periodicity and eventually up to the situation of the incident individual IR laser beam.

#### 4. Conclusions

We have studied the formation of subwavelength dot-like matrix surface structures on Mo plate by irradiating two-color femtosecond laser beams (50 fs,  $\lambda = 800$  nm and 400 nm). The main points can be summarized as follows: (i) With direct irradiating collinear two-color laser beams out of BBO crystal, 2D periodic arrays of dot surface structures have been fabricated in a single translation step. Both structure periodicities and orientations can be modified with different laser parameters. (ii) With varying the delay time of two-color femtosecond laser beams, we have clearly identified that the formation of dot-matrix structures is physically based on the transient correlation of the dual laser-matter interactions through modifying their ultrafast surface dynamics, rather than a simple intersection of two orthogonal LIPSSs individually from two-color beams. (iii) Relying on the transient correlated actions, the dot-matrix structures can be transformed into different types, even with great reduction of the periodicity by half at certain delay times. The discussion might suggest a new way for fabricating, controlling and optimizing complex nanoscale surface structures on the metal surfaces towards their potential applications in plasmonic devices, chemical catalysis and energy storage technology.

#### Acknowledgments

We acknowledge financial supports from the National Science Foundation of China (grant no. 11274184), the Tianjin National Natural Science Foundation (grant no. 12JCZDJC20200) and the Research Fund for the Doctoral Program of Higher Education of China (grant no. 20120031110032)